

Liquid-solid phase transition in a confined granular suspension

Nariaki Sakaï,* Sébastien Moulinet, and Frédéric Lechenault
*Laboratoire de Physique Statistique, Ecole Normale Supérieure,
 PSL Research University, UPMC, CNRS, 75005 Paris, France*

Mokhtar Adda-Bedia
*Univ. Lyon, ENS de Lyon, Univ. Claude Bernard,
 CNRS, Laboratoire de Physique, F-69342 Lyon, France*
 (Dated: 10 janvier 2017)

We experimentally investigate the phase behaviour of a model two-dimensional granular system undergoing stationary sedimentation. Buoyant cylindrical particles are rotated in liquid-filled drum, thus confined in a harmonic centripetal potential with tunable curvature, which competes with gravity to produce various thermal-like states : the system can be driven from liquid-like to solid-like configurations as the rotation rate is increased. We study the statistics of the local hexagonal order across this transition, which exhibits large fluctuations and heterogeneities as the dense phase of the system develops spatial ordering. In particular, the spontaneous appearance of locally crystallized regions in the disordered phase points to the existence of an underlying critical point : size distribution displays scale invariance when approaching the transition, which in turn occurs when the packing fraction crosses the random close packing. This suggests that the ordering transition is only due to geometrical effects, in contrast with other experiments on liquid-solid phase transition of granular media. Finally, a simple force balance explains when the perfect crystalline state occurs yielding an upper bound for the critical frequency of the transition.

PACS numbers: 83.80.Hj, 47.57.E, 47.57.Gc

Statistical approaches to the phase behavior of granular matter have flourished during the past twenty years, from kinetic theories to Edwards hypothesis, culminating with the jamming paradigm [1]. However, no unifying framework has emerged that captures the physics of this class of systems the way thermal statistics do for molecular systems. Energy dissipation and athermality are two defining features of granular matter : since thermal fluctuations are irrelevant for millimeter-sized particles, achieving a dynamical steady state requires a continuous energy injection to compensate for the dissipative processes. This usually takes the form of a mechanical agitation which plays the role of the thermal bath. When this is achieved, particles behave like a fluid, and for 2D monodisperse systems, the granular fluid crystallizes when the density of particles is increased [2–6]. The transition also occurs by cooling the system *i.e.* decreasing the mean kinetic energy by decreasing the injected power [5, 7–9]. Particles can also interact with each other through electrostatic [10] or magnetostatic [11, 12] interactions, in which case it is possible to obtain a transition by tuning the strength of the interaction. These observations are very similar to what is observed in simulations of hard disks with elastic collisions [13, 14, 17], or for colloidal systems [15–18], despite the fact that granular fluids are out of equilibrium. However, the depth of this analogy remains elusive, partly due to dissipative processes like solid friction, *e.g.* the so-called granular temperature does not equilibrate between phases when there is coexistence [7]. This leads to question to what extent concepts from thermodynamics can be exported to these out of

equilibrium situations [9, 19–22].

On the one hand, most of the experimental studies on dense granular media and their liquid-solid phase transition have been carried out by controlling the packing fraction, *e.g.* by changing the number of particles in a given fixed volume with hard walls [4]. On the other hand, simple granular sedimentation experiments cannot be sustained within dynamical steady-states for long enough to decipher the resulting statistical ensemble they evolve in. Here we present an experimental situation where a buoyant granular suspension is instead confined in a harmonic trap with tunable curvature and maintained in a continuous sedimentation state. In addition to gravity effects induced by the mismatch in density between the fluid and the grains, a centripetal confining pressure is adjusted by changing the rotation rate of the system. The competition between this confinement and buoyancy allows to select the density profile of the assembly and thus to explore various packing states. Furthermore, instead of solid friction, the particles are coupled through hydrodynamic interactions. Altogether, the system can be continuously driven from a dispersed to a crystalline state, undergoing in particular a disordered to ordered phase transition.

In this Letter, we study the transition of the system from a loose liquid-like state towards an ordered crystal as a function of the confinement. We first focus on the spatial arrangement of particles in the harmonic trap, and characterize the transition by the so-called bond-orientational order parameter. We find that the mean size of monocrystalline regions grows sublinearly beyond

a critical rotation rate at which the spatial distribution of the structure is maximally heterogeneous. The size distributions of these regions display scale invariance in the vicinity of this rotation rate. Furthermore, the cut-off size of these distributions scales with the distance to random close packing, confirming the critical nature of the transition. Finally, we discuss the mechanism of the transition as the onset and equilibration of internal forces and interpret the value of the critical packing fraction as the random close packing.

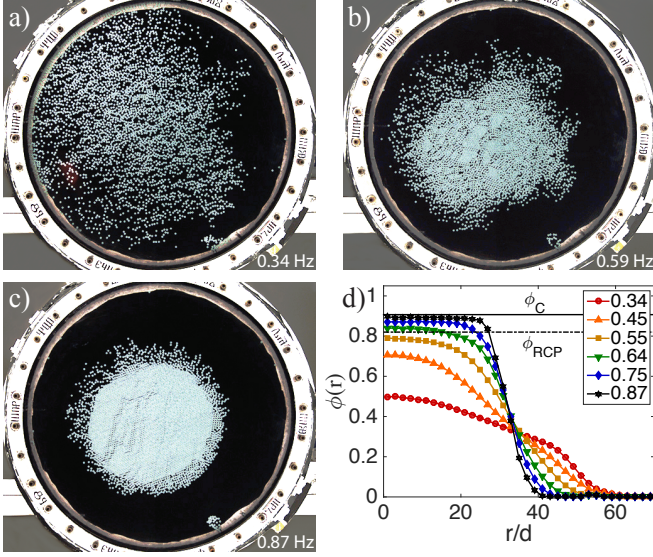


FIGURE 1. Snapshots of the system at different rotation frequencies : (a) 0.34Hz, (b) 0.59Hz and (c) 0.87Hz. Note that for the latter, the system is composed of a monocrystal surrounded by a gaseous phase. (d) Mean packing fraction profiles at 6 values of rotation rates (in Hz). The dashed horizontal line corresponds to the random close packing and the bold line to the crystal packing fraction.

The experimental setup is inspired from [23]. It consists in putting a monolayer of $N_0 \approx 3800$ cylindrical particles of diameter $d = 4\text{mm}$, height $h = 2\text{mm}$ and density $\rho = 1.01 \times 10^3 \text{kg} \cdot \text{m}^{-3}$ in a two-dimensional cylindrical drum of radius $R_0 = 250\text{mm}$. The two parallel plates of the drum are separated by a distance $1.5h$ and the cell is filled with a solution of cesium chloride of density $\rho_l = 1.55 \times 10^3 \text{kg} \cdot \text{m}^{-3}$, making the liquid denser than the particles. The axis of the cell is horizontal, so particles feel the effect of gravity, and the system is rotated with a motor (ABB Motors) at a frequency f ranging from 0.35Hz to 0.95Hz. A high resolution camera (SVS Vistek) is placed in front of the cell and triggered by means of an optical fork once every cycle. We focus on the statistics of the packing computed over a series of 2000 pictures per value of the rotation rate. Particles are hollow cylinders made of white polystyrene and filled with a green silicon core, in order to ease their detection : error on the positions is of the order of $20\mu\text{m}$.

The phenomenology of this system is quite rich : at very low rotation rate, the grains float up to the top of the cell and avalanche similarly to what occurs in a partially filled rotating drum [24], a regime we do not study here. Three pictures of the experiment at different rotating rates are shown in Fig. 1 ; they correspond respectively to the fully dispersed state where the interparticle distance is larger than the grains diameter, the state near the critical point where a dense, disordered region has invaded a significant central region, and finally a state with a large ordered crystal in the center of the cell surrounded by a gas-like ring. An illustrative movie of the different phases is provided in [25].

Let us now detail the physical ingredients at play within the system. The rotation of the cell creates a radially linear outward pressure gradient for the buoyant particles, resulting in a centripetal force. On top of this rotationally symmetric potential, gravity pushes on the particles upwards. Interestingly, the coupling to the fluid in this Hele-Shaw geometry yields a strong drag on the grains, which in the regimes of interest tend to co-rotate with the cell. Thus in the rotating frame, gravity is a spinning force that tends to disperse the particles outwards, competing with the confining potential and injecting power into the system. Changing the rotation rate shifts the balance between these forces. In the polar coordinate system ($\vec{e}_r, \vec{e}_\theta$) associated with the laboratory frame, the equation of motion of a single grain reads :

$$\rho V \frac{d\vec{v}}{dt} = \mu(\vec{v} - \omega r \vec{e}_\theta) + (\rho - \rho_l)V\vec{g} - \rho_l V \omega^2 r \vec{e}_r, \quad (1)$$

where $\omega = 2\pi f$ is the rotation rate, μ is the viscous drag coefficient measured to be $1.1 \times 10^{-3} \text{Nm}^{-1}\text{s}$ in the experiment, V is the volume of the particle, r is the radial position of its center of mass away from the center of the cell and \vec{v} is its velocity. Interestingly, this equation admits a fixed point solution (r^*, θ^*) given by $r^* = l_c \sin \theta^*$ and $\tan \theta^* = -\frac{\rho_l \omega}{\mu V}$, with $l_c = \frac{(\rho_l - \rho)g}{\rho_l \omega^2}$ being defined as the confinement length. Thus the trajectory of a single particle in an infinite system would spiral towards this point for all finite rotation rates. However, due to the collective nature of the system, the hydrodynamic coupling between particles at the intermediate Reynolds numbers at hand tends to spread them apart, as verified independently through additional two-particle sedimentation experiments, resulting in the observed stationary dispersed states.

To characterize the spatial distribution of particles in the cell, we first compute the mean packing fraction $\phi(r) = \langle dA(r)/2\pi r dr \rangle$ where $dA(r)$ is the cumulated area of the particles located in a ring of width dr at distance r from the instantaneous centre of mass of the grains, which does not coincide with the center of the cell. This quantity is displayed in Fig. 1(d). At low frequency, this profile is roughly parabolic. However, at $f \approx 0.4\text{Hz}$, the packing fraction starts to develop a plateau at the

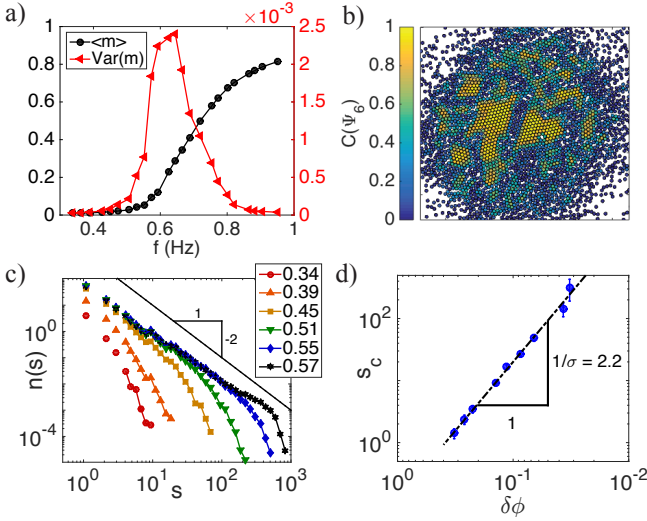


FIGURE 2. (a) Time average and variance of the order parameter $m = |1/N_0 \sum_{k=1}^{N_0} \psi_6^k|$. (b) Instantaneous configurations of the system at $f = 0.59$ Hz, where particles are patched with a color corresponding to the value of the first neighbors correlation $C(\psi_6)$. Particles which are crystallized are yellow (bright) in contrast with particles in a disordered phase which are blue (dark). (c) Size distributions of monocystals for different values of the rotation frequency. (d) Characteristic cut-off size of these distributions as a function of the distance to ϕ_{RCP} .

center as frequency is increased, corresponding to a dense region where particles are in contact. At high rotation rates $f > f_{crys} \approx 0.8$ Hz, the value of the plateau tends to the packing fraction of the crystal $\phi_c = \pi/\sqrt{12} \approx 0.9$ as the assembly fully orders.

The characterization of the state of the granular assembly is monitored using the bond-orientational order parameter ψ_6^k [14]. For each particle k , one defines $\psi_6^k = 1/N_k \sum_{l=1}^{N_k} e^{6i\theta_{kl}}$, where the sum runs over all first neighboring particles l and θ_{kl} is the angle between the line from particles k to l and a globally fixed arbitrary axis - the neighbors are found by computing the Voronoi diagram from the particles positions. For particles in a hexagonally ordered neighborhood, $|\psi_6| = 1$. Moreover, this quantity is constructed such that its phase is the same for all particles in the same monocrystal. In order to capture the global state of the system, we define a monocrystalline order parameter as $m = |1/N_0 \sum_{k=1}^{N_0} \psi_6^k|$, where the sum runs over all particles in the system. The time average and variance of this quantity are shown in Fig. 2(a). At low rotation rates, the time average is constant and not significantly different from zero. It starts rising around $f = 0.4$ Hz and tends towards $m \approx 0.8$ at high rotation rates. Notice that if all the grains were in a crystalline state, one should have $m \approx 1$, however even for the highest frequency we probed one is still left with a thin layer of grains in the liquid state which makes the order parameter $m < 1$. Moreover, fluctuations of this order parameter are close to zero at low

and high rotation rates, but sharply rise and pass through a maximum at $f_c \approx 0.64$ Hz, much like in the vicinity of a critical point.

If two particles belong to the same monocrystal, the orientations of their ψ_6 are the same. Thus, in order to be able to distinguish between neighboring ordered regions with different orientations, we define for every particle k the first-neighbor correlation $C(\Psi_6^k) = \psi_6^k \cdot \langle \psi_6^l \rangle_l$ which is the scalar product of the bond-orientational order parameter of the particle k and its first neighbors - the average $\langle \cdot \rangle_l$ is taken over all first neighbors l and we express the correlation by taking the vectorial form of the complex number ψ_6 . A snapshot of the particles distribution at the transition is displayed in Fig. 2(b). When the system approaches this ordering transition from the disordered state, many locally crystallized clusters appear in the liquid phase. These clusters are intermittent and grow in size when the system approaches the transition. Above the transition frequency, they percolate to form a unique connected region, but heterogeneities continue to be large, as embodied by the rugosity and fluctuations of the interface between the monocrystal and its surroundings. When the system is driven away from the transition point, this rugosity decreases and the monocrystal becomes circular, where interface fluctuations are only due to adsorption and desorption of particles at the interface.

In order to quantify these heterogeneities, we measure the size s and perimeter p of the crystalline clusters. They are defined as ensembles of Voronoi neighbors that all have $C(\psi_6)$ larger than a given threshold fixed at 0.5. We have checked that the results are insensitive to a variation of a thresholding around this value. Size and perimeter correspond respectively to the number of particles in the cluster and on its boundary. First, we find that approaching the transition from the disordered side, the size distribution of these clusters displays a power-law regime stretching further towards larger sizes as the transition is approached, as can be seen in Fig. 2(c). This scale invariance developing in a finite region around the transition is a clear indication of criticality. Furthermore, we find that in this parameter range, the relation between the size and perimeter of the clusters is also a power law with a non-trivial roughness exponent $s \propto p^{1.2}$ (Fig. 3(a)). As the rotation rate is further increased, the unique monocrystalline region that crosses the system continues to grow in size, but its perimeter now decrease, resulting in a vanishing roughness: at high rotation rates, sizes and perimeters are just related by $s = p^2/4\pi$ which corresponds to a perfect circular shape, as emphasized in Fig. 3(a). In the same spirit, we have computed the radius of gyration of each cluster s as given by $R_g^2(s) = 1/s \sum_{k=1}^s (\vec{r}_k - \langle \vec{r}(s) \rangle)^2$. Fig. 3(b) shows that the cluster size is a power-law function of R_g with an exponent $d_f \approx 1.8$, as one would expect from a percolation-like transition.

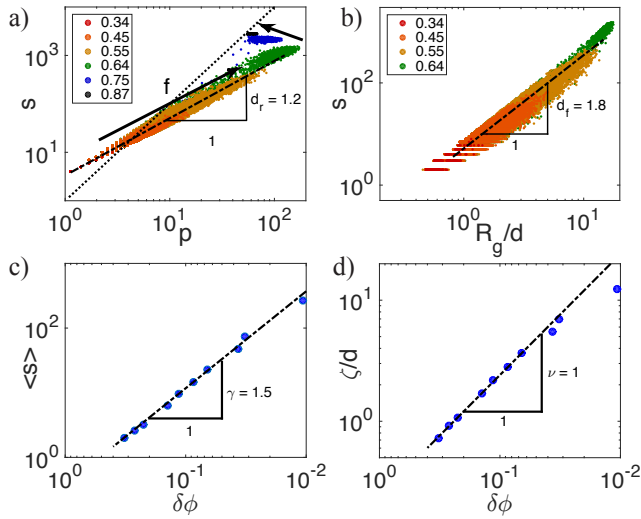


FIGURE 3. (a) Scatter plot of size s vs. perimeter p of the clusters for rotation frequencies ranging from 0.34Hz to 0.9Hz. Each point correspond to one cluster and each color correspond to a given rotation rate. When the rotation rate is increased (arrows), sizes and perimeters of clusters in the liquid phase grow according to a power law with a non-trivial exponent $d_r \approx 1.2$. After the transition, the system is composed of a unique crystallized region. Its roughness decreases and departs from the $s \propto p^{1.2}$ law (solid line) to reach $s = p^2/4\pi$, (dotted line) which corresponds to a circular compact region. (b) Scatter plot of the cluster size versus the radius of gyration of the clusters. (c) Average cluster size $\langle s \rangle$ and (d) correlation length ζ versus the packing fraction difference $\delta\phi$.

Interestingly, at the transition frequency $f_c \approx 0.64\text{Hz}$, the packing fraction at the center of mass of the granular suspension reaches $\phi = 0.82 \approx \phi_{RCP}$, the random close packing density, a value that is much larger than the *solidus* point in both thermal [13, 14] and athermal [4] hard disks. In order to further assess the critical nature of the transition at hand, we computed additional quantities that usually scale with the distance of the control parameter to the critical point. First, Fig. 2(d) shows the cut-off size s_c when the cluster size distributions $n(s)$ is fitted by $n(s) = s^{-\tau} \exp(-s/s_c)$. Though s_c doesn't exhibit any particular behaviour when plotted against other quantities, it appears to scale with the distance of the packing fraction to the random close packing, $\delta\phi \equiv \phi_{RCP} - \phi(r=0)$, with an exponent close to 2.2. Furthermore, Fig. 3 (c,d) confirm that the average cluster size $\langle s \rangle = \sum_s s^2 n_s / \sum_s s n_s$ and the correlation length ζ , as given by $\zeta^2 = 2 \sum_s R_s^2 s^2 n_s / \sum_s s^2 n_s$ [26], also exhibit scaling properties as function of $\delta\phi$, with exponents respectively close to 1.5 and 1.

The state of the granular suspension is governed by the competition between the harmonic centripetal confinement, gravity and the hydrodynamic coupling between the liquid and the grains. The viscous drag regulates the energy content in the assembly. At low rotation rate, the

confinement is sufficiently loose to enable the buoyancy to disperse the grains across the cell, whereas at higher rotation rates it becomes strong enough to bring some of the grains to contact (cf. Eq. 1). When the grains are packed in a perfect crystalline state, there is equilibration of the two forces at the boundary of the crystal, which starts being able to sustain internal stress. This transition occurs typically when the confinement length $l_c = \frac{(\rho_l - \rho)g}{\rho_l \omega^2}$ becomes comparable to the typical radius $R \approx (d/2)\sqrt{N_0/\phi_c}$ of the crystalline phase. This leads to an estimate $f_{cryst}^{est} = 0.82\text{Hz}$ of the frequency at which a crystal is formed, which is reasonably close to the measured value $f_{cryst} \approx 0.8\text{Hz}$ and leads to an upper bound for the critical frequency $f_c \approx 0.64\text{Hz}$.

In summary, we report an experimental study of a liquid-solid-like phase transition in a two dimensional granular suspension in which the state of the system is controlled by applying an adaptive confinement. The transition is controlled by the competition between the buoyancy and the centripetal force which allows us to relate the critical rotation rate with the parameters of the experiment. The behavior of assembly is well described by the global bond-orientational order parameter $m = |1/N_0 \sum_{k=1}^{N_0} \psi_6^k|$ which time average is zero in the liquid-like phase and non-zero for the solid, and which fluctuations peak around a transition frequency $f_c = 0.64\text{Hz}$. This means that near the transition, large heterogeneities develop within the system through the appearance of many small monocrystals. In this disordered phase, sizes and perimeters of these clusters obey geometrical scaling relations, and display a critical behaviour with respect the distance to random close packing, which thus appears as a critical point. Future work in deciphering this system's statistics will focus on its dynamics, since it appears to be undergoing a coupled shear flow pattern. Large deviations of the packing fraction and kinetic energy are also under scrutiny, in the hope to extract relevant state functions related to the aforementioned criticality.

* nariaki.sakai@lps.ens.fr

- [1] A. J. Liu and S. R. Nagel, *Annu. Rev. Condens. Matter Phys.* **1**, 347 (2010).
- [2] G. Strassburger and I. Rehberg, *Physical Review E* **62**, 2517 (2000).
- [3] S. C. Wu, D. T. Wasan, and A. D. Nikolov, *Physical Review E* **71**, 1 (2005).
- [4] P. M. Reis, R. a. Ingale, and M. D. Shattuck, *Physical Review Letters* **96**, 4 (2006), [arXiv :0603408 \[cond-mat\]](https://arxiv.org/abs/0603408).
- [5] F. V. Reyes and J. S. Urbach, *Physical Review E* **78**, 1 (2008), [arXiv :0803.1158](https://arxiv.org/abs/0803.1158).
- [6] Y. Komatsu and H. Tanaka, *Physical Review X* , 8 (2015), [arXiv :1509.03435](https://arxiv.org/abs/1509.03435).
- [7] A. Prevost, P. Melby, D. a. Egolf, and J. S. Urbach,

- Physical Review E **70**, 1 (2004), arXiv :0312232 [cond-mat].
- [8] J. S. Olafsen and J. S. Urbach, *Physical Review Letters* **95** (2005), 10.1103/PhysRevLett.95.098002, arXiv :0501028 [cond-mat].
 - [9] G. Castillo, N. Mujica, and R. Soto, *Physical Review Letters* **109**, 1 (2012), arXiv :1204.0059v1.
 - [10] X. H. Zheng and R. Grieve, *Physical Review B* **73**, 1 (2006).
 - [11] J. Schockmel, E. Mersch, N. Vandewalle, and G. Lumay, *Physical Review E* **87**, 1 (2013).
 - [12] S. Merminod, M. Berhanu, and E. Falcon, *Europhysics Letters* **106** (2014), 10.1209/0295-5075/106/44005.
 - [13] W. Qi, A. P. Gantapara, and M. Dijkstra, *Soft Matter* **10**, 5449 (2014), arXiv :1307.1311v2.
 - [14] E. P. Bernard and W. Krauth, *Physical Review Letters* **716** (2011), 10.1103/PhysRevLett.107.155704, arXiv :1102.4094.
 - [15] A. H. Marcus and S. A. Rice, *Physical Review Letters* **77**, 2577 (1996).
 - [16] P. Keim and G. Maret, *Physical Review E* **75**, 2 (2007).
 - [17] Z. Wang, A. M. Alsayed, A. G. Yodh, and Y. Han, *Journal of Chemical Physics* **132** (2010), 10.1063/1.3372618.
 - [18] P. Dillmann, G. Maret, and P. Keim, *Journal of Physics : Condensed Matter* **24**, 464118 (2012), arXiv :1210.3966.
 - [19] G. D’Anna, P. Mayor, a. Barrat, V. Loreto, and F. Nori, *Nature* **424**, 909 (2003), arXiv :0310040 [cond-mat].
 - [20] R. P. Ojha, P.-a. Lemieux, P. K. Dixon, a. J. Liu, and D. J. Durian, *Nature* **427**, 521 (2004).
 - [21] J. G. Puckett and K. E. Daniels, *Physical Review Letters* **110**, 1 (2013), arXiv :1207.7349.
 - [22] L. H. Luu, G. Castillo, N. Mujica, and R. Soto, *Physical Review E* **87** (2013), 10.1103/PhysRevE.87.040202, arXiv :1209.2837v2.
 - [23] E. Bayart, A. Boudaoud, and M. Adda-Bedia, *Physical Review E* **89**, 1 (2014).
 - [24] N. Sepulveda, G. Krstulovic, and S. Rica, *Physica A* **356**, 178 (2005).
 - [25] See Supplemental Material at [URL will be inserted by publisher] for movies illustrating the phase behavior of the experiment.
 - [26] D. Stauffer and A. Aharony, *Introduction to Percolation Theory*, 2nd ed. (Taylor & Francis, London, 1992).